PGET Monte Carlo simulations using Serpent

Topias Kähkönen[1], Ilja Makkonen[2], Riina Virta[3,4], and Peter Dendooven[3,*]

[1]*VTT Technical Research Centre of Finland*
[2]*Department of Physics, University of Helsinki, Finland*
[3]*Helsinki Institute of Physics, University of Helsinki, Finland*
[4]*The Radiation and Nuclear Safety Authority (STUK), Finland*
[*]*Corresponding author: peter.dendooven@helsinki.fi*

Abstract. Since 2017, over 100 spent nuclear fuel assemblies at the Finnish nuclear power plants have been imaged with the Passive Gamma Emission Tomography (PGET) device in preparation of the implementation of PGET in the safeguards infrastructure of the Finnish geological repository. In order to increase understanding of the PGET method and guide its further development, we have recently implemented PGET in Serpent, a widely-used neutron and photon transport Monte Carlo simulation code. We will discuss the major aspects of this implementation and illustrate the usefulness of the simulations with a few examples. The PGET device as used in the measurements (which was developed under the guidance of IAEA and is approved for safeguards inspections) was implemented in a very realistic way based on its technical drawings. The simulation produces sinograms in user-defined energy windows as well as the uncertainty on these sinograms. Tomographic images are then reconstructed using the exact same algorithm as used for the measured data. A dedicated variance reduction scheme was implemented, increasing the computational efficiency by about a factor of 30. The simulation of the PGET response at one angular measurement position for 1 billion primary photons takes a few hours on a single 40-core node. The 1-sigma uncertainty in the highest intensity sinogram pixels is about a few percent. Aiming at improving the imaging of VVER-440 assemblies, we have simulated assemblies containing one or a few missing fuel rods or having only one emitting rod (the other rods being present but not emitting) in various well-chosen places, configurations that are not accessible in practice. The single-emitting rod results show in great detail those parts of the sinogram that contain most of the information for the particular rod position. How this information might be used for obtaining better images, especially of the central region of a fuel assembly, will be discussed.

1 Introduction

Monte Carlo (MC) simulations are a common tool in radiation transport and detection problems. They can be sufficiently realistic to make instrument design decisions, reducing the need for prototyping and experimental testing. MC simulations are used as a surrogate for experiments and measurements. Simulations are often easier to perform and provide more control over a situation than experiments. More importantly, one can simulate what is physically (near) impossible or practically very difficult to measure. Simulations are thus a very good tool to gain a better understanding of radiation transport and detection devices and applications.

Serpent is a widely-used neutron and photon transport Monte Carlo simulation code, originally developed for nuclear reactor physics burnup calculations [1]. Essential for the work presented in this paper are the support for CAD-based geometries [2] and the photon transport capability [3, 4]. The photon transport model includes the four major interaction processes, namely the photoelectric effect, Rayleigh scattering, Compton scattering and pair production. Secondary photons are generated from positron-electron annihilation, atomic relaxation and as Bremsstrahlung photons of charged particles which originate from photon interactions. Electrons and positrons are relevant in photon transport. However, the current version of Serpent does not include the transport of charged particles. Instead, the interactions of electrons and positrons are modelled locally: their energy loss is assigned to the location where they are created and Bremsstrahlung photons are assumed to be created at this location. This approximation is good for photon transport in general [4], but in highly detailed smaller-scale simulations, it might not be valid.

We are using Serpent simulations in our continuing development of Passive Gamma Emission Tomography (PGET) of spent nuclear fuel. This activity is related to the Finnish national safeguards protocol for the deep geological repository of spent nuclear fuel [5], the first one in the world to become operational, planned for 2025. This protocol is developed by the Finnish Radiation and Nuclear Safety Authority (STUK) and partners such as the Helsinki Institute of Physics at the University of Helsinki. The protocol prescribes that all spent fuel assemblies will be non-destructively characterised at their interim storage pool before being transported to the encapsulation plant. PGET [6, 7] will be used to verify the presence of fuel at the level of a single rod, while a Passive Neutron Albedo Reactivity (PNAR) [8, 9] measurement will indicate the presence of fissile material. These measurement outcomes will be combined in a final safeguards assessment.

We report here on the implementation and first results of Serpent simulations for PGET of spent nuclear fuel. The general aim is to gain a better understanding of the method, which should lead to improvements in the operation of the PGET device, the analysis of its data and its image reconstruction. Additionally, improved designs may be proposed. The focus is on VVER-440 fuel as results from PGET measurements at the Loviisa nuclear power plant show that the quality of imaging the center of the assembly needs to be improved [10]. The first steps in this quality enhancement are reported in [11].

2 Methods

We use Serpent 2.1 for PGET simulations with a new variance reduction method. The distributed version of Serpent can simulate all phases of the calculation sequence, but we developed the variance reduction method to speed up the photon radiation transport. The method was tailored for this specific transport problem and it is not currently distributed with Serpent.

2.1 Calculation sequence

Figure 1 shows the general structure of the PGET calculation sequence. First, we calculate the nuclide inventory for an irradiated nuclear fuel assembly. Then, we simulate the radiation transport from the fuel to the surface of the gamma detectors using the irradiated assembly. As the PGET detectors are very small ($3.5 \times 3.5 \times 1.75$ mm^3) and electrons are not tracked, the present simulations can not accurately take the detector response into account. Therefore, we only create sinograms (2D matrix of the detector response versus detector position and viewing angle) based on the incident photon current, but we are considering to improve the detector model.

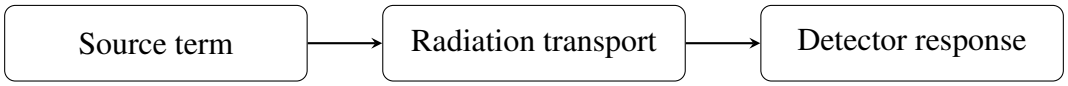

Figure 1: Illustration of the multi-phased calculation sequence. All phases of the sequence are simulated with Serpent.

We calculate the fuel nuclide inventory by simulating the irradiation in a two-dimensional infinite lattice. For a VVER-440 assembly, the approximation is achieved by applying periodic boundary conditions around the hexagonal assembly. The irradiation phase is then followed by a cooling period. We solve the burnup and decay problems with the Serpent internal burnup solver including all nuclides with available data in the JEFF 3.1.1 nuclear data library. The radiation transport phase then uses the full nuclide inventory to calculate the emission spectrum.

The geometry of the radiation transport is illustrated in Figure 2. It is based on a hybrid constructive solid geometry (CSG) and a CAD model. The fuel assembly is modelled with CSG while the PGET device uses detailed technical drawings of the device in STL format. The included CAD model contains collimators and the central part of the housing as shown in Figure 2a. The housing of the device is composed of stainless steel and the collimators are composed of tungsten. The fuel assembly is surrounded by water and the device is filled with air.

We simulate the sinogram by rotating the fuel assembly step by step and calculating the radiation transport at each angle. We measure the incident photon current behind each collimator slit. In practice, we tally the photon current with a Serpent surface current detector behind the collimators and bin it spatially in the x-direction into 0.25 mm wide bins. The total photon current behind each 1.5 mm wide slit is calculated as the sum of 6 partial currents and the associated relative statistical uncertainty s_r is calculated according to

$$s_r = \frac{s}{J} = \frac{\sqrt{\sum_{i=1}^{n} s_{r,i}^2}}{\sum_{i=1}^{n} J_i}. \tag{1}$$

Here s is the standard deviation, J is the total photon current, J_i is a partial current, $s_{r,i}$ is the relative standard deviation of the partial current, and n is the number of summed partial currents. In addition to spatial binning, we record incident photons in different energy bins according to the defined measurement energy windows.

2.2 Variance reduction

Using analog photon transport in the PGET geometry is highly inefficient and practically limits the feasibility of simulations. Therefore, we implemented a new variance reduction method in Serpent specifically for this application. In addition, the efficiency of the simulation is increased by eliminating photon histories below the energy interval of interest.

The development of the new method was influenced by existing methods in other codes called forced detection [12, 13, 14] and convoluted forced detection [14, 15]. The method splits photons into several fragments at selected interactions and samples photon fragments in specified directions, hence the name directional splitting. The goal of the method is to increase the sampling rate of photon histories passing through the collimator slits.

Figure 3 illustrates the idea of directional splitting. Splitting calculates weights for directed particles proportional to the probability of actually sampling the incident particle inside solid angles Ω_1 and Ω_2. The weight for the undirected particle is calculated from the residual conserving the total weight balance.

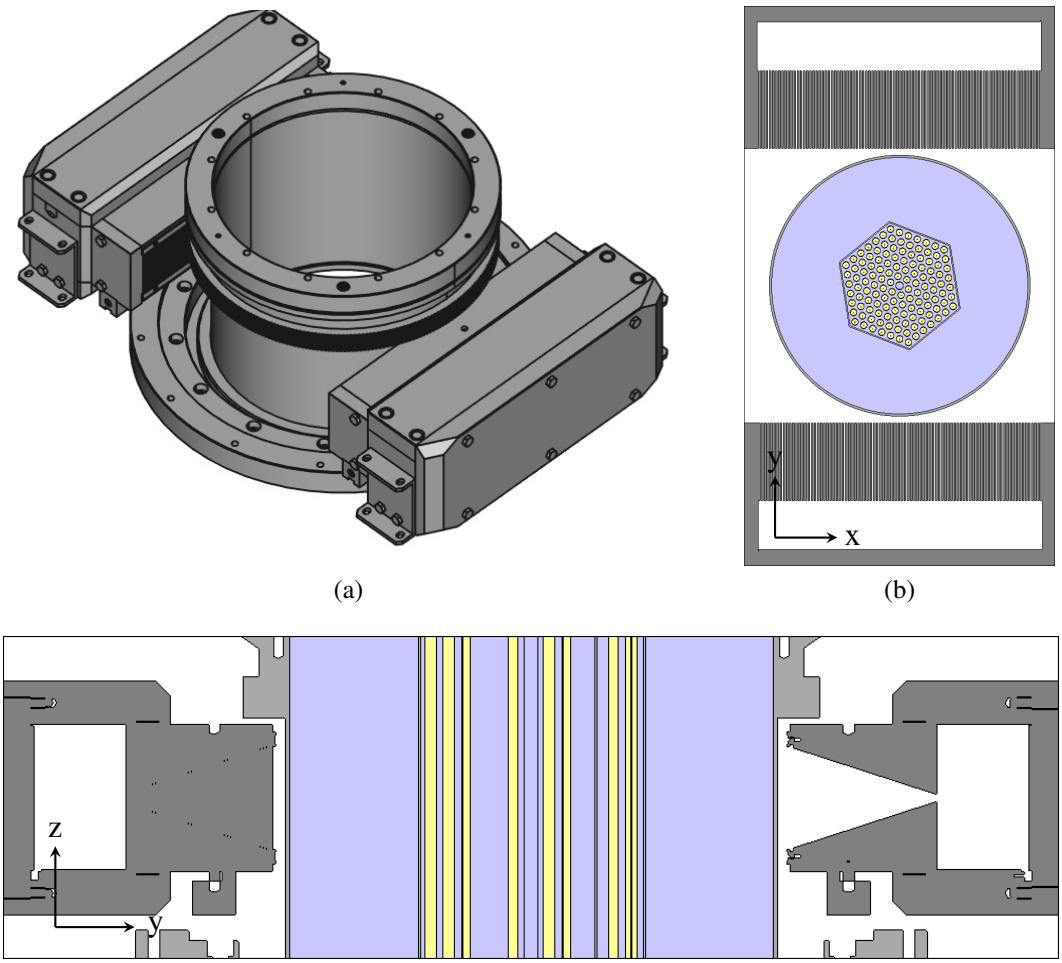

(a) (b) (c)

Figure 2: CAD-based model of the PGET device (a) and cross-section images of the whole Serpent geometry (b and c). (b) shows the center-line cross-section in the xy-plane and (c) shows the cross-section in the yz-plane. Dimensions in the x, y, and z directions are 40 cm, 72 cm, and 22 cm, respectively.

We implemented directional splitting for Compton scattering and for the photon emission from the source. These are the most important phenomena affecting the direction of photons in the specific transport problem. The weight for directed particles from an isotropic decay source can be calculated from the ratio of the solid angle of the directed cone and the full solid angle. However, calculating weights for Compton scattering requires more intermediate steps.

Serpent uses the Klein-Nishina formula multiplied by the incoherent scattering function to model the distribution of scattering angles in Compton interaction [4]. Therefore the weight of a directed photon has to be calculated according to

$$w = \frac{1}{\sigma_{co}} \int_{\Omega'} \left(\frac{d\sigma_{co}}{d\Omega} \right)_{KN} S(q, Z)\, d\Omega. \tag{2}$$

Here w is the weight of the directed particle fragment, σ_{co} is the Compton microscopic cross section, $\left(\frac{d\sigma_{co}}{d\Omega}\right)_{KN}$ is the Compton double differential cross section according to the Klein-Nishina formula, and $S(q, Z)$ is the incoherent scattering function. It suppresses forward scattering especially for heavy elements, hence it depends on the atomic number Z of the target element and the momentum transfer vector q.

The weights for photon emission are calculated on the fly but the weights for Compton scattering are calculated before the transport. The integral in Equation (2) is evaluated numerically over the solid angle Ω' bounded by the directed cone. The weights are then tabulated for different elements and scattering angles. The directional splitting routine reads pre-calculated weights from the table with linear interpolation.

The use of directional splitting leads to a heavily branching photon tracking routine. However, the weight of directed particles reduces significantly after each splitting event, and tracking photons with extremely small weights is inefficient. Hence, we use Russian roulette with a fixed weight limit set at $1.5 \cdot 10^{-2}$ to prune particles with small weights after directional splitting. The limit is of the same magnitude as particle weights after the first splitting event.

Photon fragments from the directional splitting have significantly varying statistical weights. The statistical weight of the undirected photons are close to the initial weight, but the weight of the directed photons can be several orders of magnitudes smaller. If a tally is scored with both heavy and light photons, the total variance is dominated by the variance of photons with high statistical weight. Hence, mixed contributions from directed and undirected photons will deflate benefits from the directional splitting routine.

Our approach to overcome the challenge of mixed contributions from heavy and light photons is to select conservative half angles for directed cones and ignore the contribution of undirected photons. In a sense, photons with a high statistical weight compared to directed photons are filtered from the results. The half angle for the photon source was selected to be 10.0°and for Compton scattering to be 5.7°. Filtering will lead to biased results, but the magnitude of the bias can be estimated from the scores of heavy photons.

Because the directional splitting was implemented only for a photon decay source and Compton scattering, other physical phenomena altering the photon direction will be ignored with heavy particle filtering. Additionally, particles penetrating the collimator beyond the acceptance angle of slits are ignored. Hence, the directional splitting accompanied with heavy particle filtering is valid only if the effects from Rayleigh scattering and pair production are not significant and particles penetrating the collimator elsewhere than at the slits can be ignored.

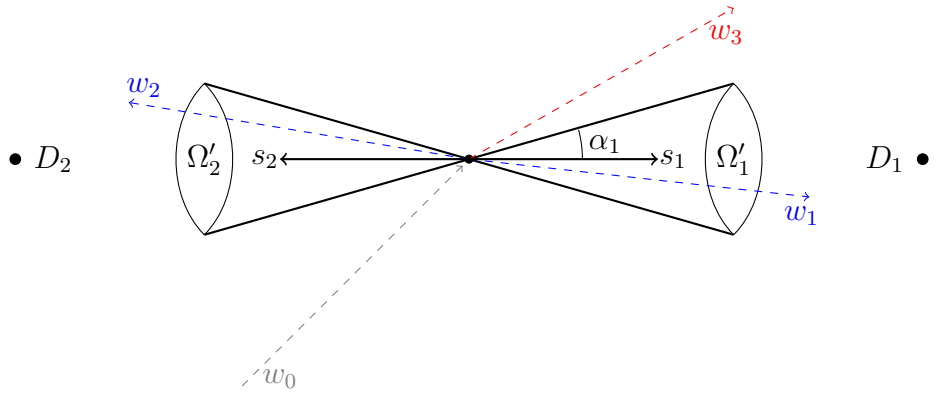

Figure 3: Illustration of the directional splitting variance reduction scheme. The incident photon with initial weight w_0 is divided at a collision site into directed and undirected fragments. Directed fragments with weights w_1 and w_2 are sampled uniformly within cones centered around vectors s_1 and s_2. The cone size is determined by the half angle α_1 and the cones are directed towards detectors D_1 and D_2. Solid angles Ω_1' and Ω_2' are used to calculate directed fragment weights. The undirected photon fragment with weight w_3 is sampled outside the directed cones with the rejection method. Each fragment is tracked normally after splitting.

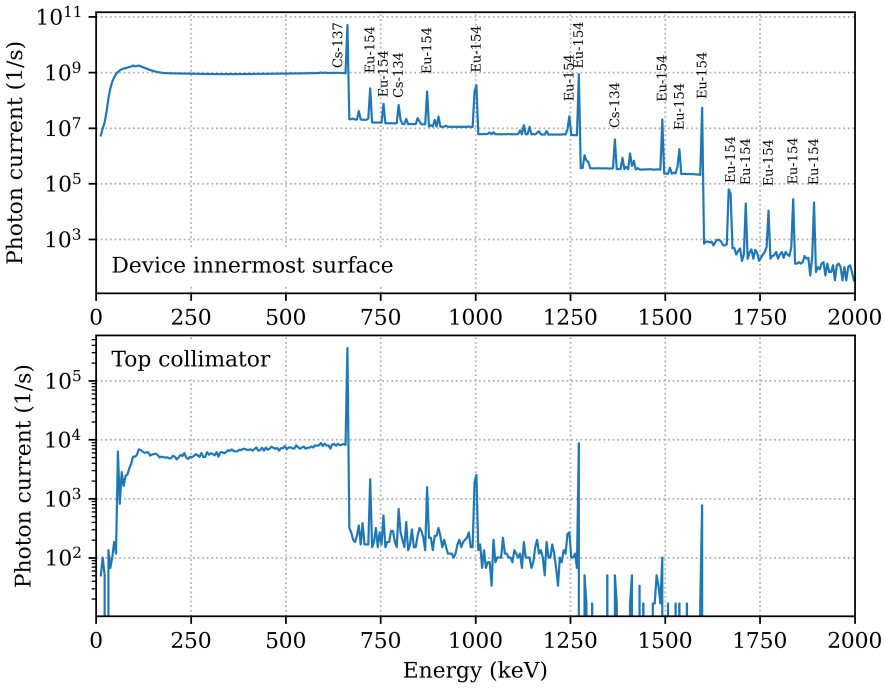

Figure 4: Energy spectra of the gamma ray photons hitting the innermost surface of the PGET donut (top) and the detectors behind the collimator slits (bottom). Only the top collimator that is shown in Figure 2b is considered, but both collimators have nominally identical spectra. In the top spectrum, the gamma ray lines are labelled with the emitting radioactive nuclide.

3 Results

3.1 Energy spectra

For a VVER-440 assembly, burnup to 50 MWd/kgU followed by a cooling time of 25 y was simulated. The resulting gamma ray emission was used as gamma emission source for a subsequent PGET simulation. During this simulation, two energy spectra were stored: the photons hitting the innermost surface of the PGET donut structure and the photons hitting the CZT detectors behind the collimator slits, see Figure 4. The first spectrum is essentially the spectrum hitting the front of the collimator, so comparing these two spectra gives insight on what kind of effect the collimator has on the gamma ray energy distribution. The overall shape and features of the two spectra are quite similar, indicating that the collimator does not significantly downscatter the gamma rays to lower energies, but largely absorbs the gamma rays.

The gamma ray source for this simulation has a 662 keV emission rate of 1.39×10^{12}/s. The intensity of the 662 keV full energy peak for one collimator is 4×10^{5}/s, resulting in an efficiency of about 6×10^{-7} for the transmission through either one of the collimators of a full energy 662 keV gamma ray. A similar calculation for the 1274 keV gamma ray gives an efficiency of about 2×10^{-6}. This 3 times higher efficiency compared to 662 keV is due to the smaller attenuation coefficient for the 1274 keV gamma rays.

Obviously, the number of gamma rays hitting the detectors is much smaller than the number of gamma rays that exit the fuel assembly and hit the innermost surface of the PGET donut: for good spatial resolution, the collimator has very long and narrow slits which have a very poor efficiency. The efficiency that a 662 keV gamma ray which exits the fuel assembly makes it through one

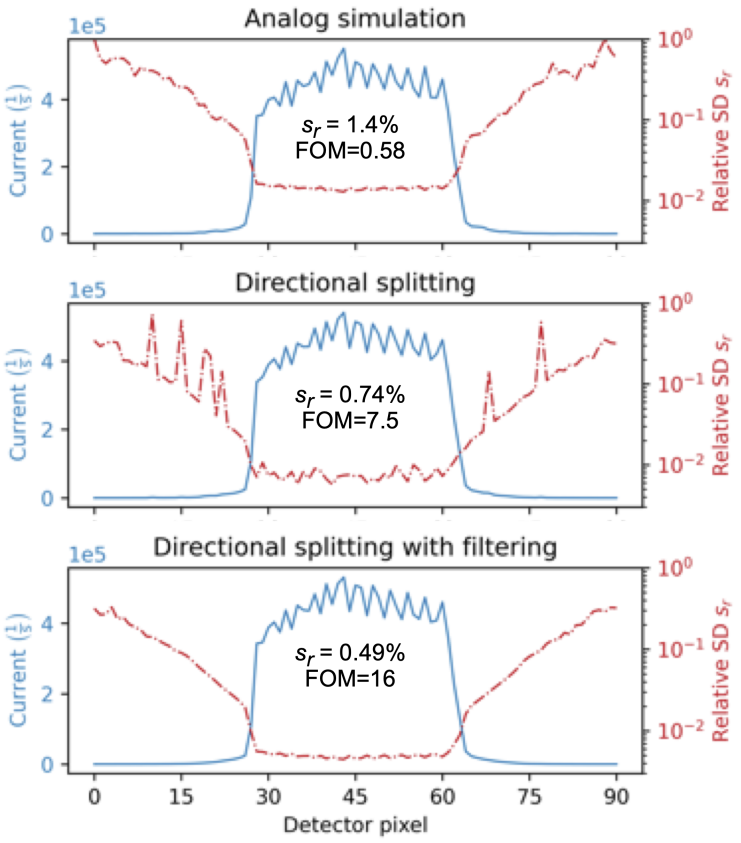

Figure 5: Photon currents and their relative standard deviations (SD) behind the collimator slits in the 600-700 keV energy window. Results are presented for the simulation without variance reduction ("analog") and simulations using directional splitting without and with filtering of large-weight photons. The relative standard deviation s_r and FOM in the region of the fuel assembly (detector pixels from 30 to 60) are given.

of the collimator slits without interaction is the ratio of the full energy peaks in both spectra: $2(4\times10^5)/(5\times10^{10})=1.6\times10^{-5}$. Both collimators are taken into account by the factor 2 in the denominator.

3.2 Validation and efficiency of variance reduction

The efficiency of the variance reduction method was investigated by comparing simulations without and with variance reduction, see Figure 5. Now and then, the directional splitting procedure attributes a very large weight to a photon. These "heavy" photons cause "spikes" in the variance of the results (see Figure 5 middle), and are therefore filtered out from the simulation (the result is shown in Figure 5 bottom). The photon currents of the three simulations are quantitatively consistent and the relative standard deviation decreases due to variance reduction, validating the variance reduction method.

The efficiency of variance reduction was evaluated by the following figure of merit (FOM):

$$\mathrm{FOM} = \frac{1}{s_r^2 T}, \tag{3}$$

where s_r^2 is the relative variance and T is the running time of the simulation. For the simulations

whose results are shown in Figure 5, the FOM increases by a factor of almost 30 when using the directional splitting with the filtering variance reduction method.

By definition, filtering reduces the number of photons that contribute to the output of the simulations. The mean effect is about 1.5%. We consider this acceptable for the purpose of the simulations, considering that filtering maintains the important physics.

3.3 A single emitting fuel rod

We show here an example of how a Monte Carlo simulation can be used to investigate a situation that can practically speaking not be realised in experimental practice. Related to investigating the imaging of the central part of a fuel assembly, it is interesting to investigate the contribution to the sinogram from centrally located spent fuel rods. Figure 6 shows the results of a Serpent simulation considering a full VVER-440 fuel assembly, but with only 1 fuel rod next to the central water hole emitting gamma rays. The sinogram shows that at certain angles, when looking head-on at one of the corners of the assembly, no gamma rays are detected. This is due to strong absorption, because at this angle gamma rays have to travel through the centre of 5 fuel rods in order to reach the detector. Interestingly, the sinogram shows maximum count rates just next to the head-on angles, because these views provide a direct line of sight to the centre of the assembly. We are further investigating, using both simulations and measurements, how this effect can be used to improve imaging of the centre of a fuel assembly. Some first measurement results are discussed in [11].

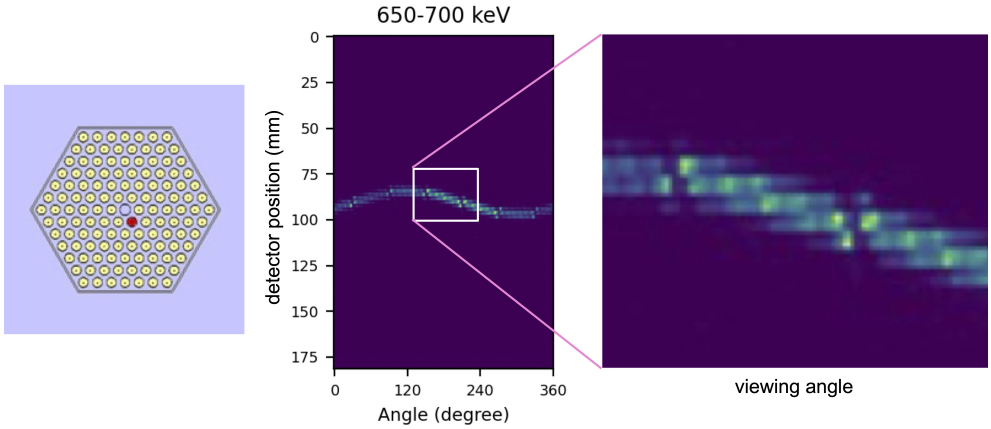

Figure 6: Results of a Serpent simulation considering a full VVER-440 fuel assembly, but with only 1 fuel rod next to the central water hole emitting gamma rays. The sketch of a VVER-440 assembly on the left highlights the emitting fuel rod. In the middle, the resulting sinogram is shown. The right image zooms in on a part of the sinogram. See the text for more details.

4 Conclusion and outlook

The Monte Carlo transport code Serpent was used to simulate the imaging of spent nuclear fuel with the PGET device. The variance reduction technique that was implemented decreases the calculation time for constant relative variance by a factor of close to 30. The simulation of a single emitting rod in the middle of a non-emitting fuel assembly illustrates the power of the simulations to improve the understanding and further development of the PGET method.

The simulation framework is now ready for routine use. Comparison with measured data is planned. However, this requires that the detector response is taken into account, either by using the Serpent output as input to a Monte Carlo code that tracks electrons in detail or by convolution of the Serpent output with an energy-dependent detector response function.

Acknowledgements

The authors wish to acknowledge CSC – IT Center for Science, Finland, for computational resources.

References

[1] Jaakko Leppänen, Maria Pusa, Tuomas Viitanen, Ville Valtavirta, and Toni Kaltiaisenaho. The Serpent Monte Carlo code: Status, development and applications in 2013. *Ann. Nucl. Energy*, 82:142–150, 2015.

[2] Jaakko Leppänen. Methodology, applications and performance of the CAD-based geometry type in the Serpent 2 Monte Carlo code. *Ann. Nucl. Energy*, 176:109259, 2022.

[3] Toni Kaltiaisenaho. Implementing a photon physics model in Serpent 2. Master's thesis, Aalto University, Espoo, Finland, aaltodoc.aalto.fi/handle/123456789/21004, 2016.

[4] Toni Kaltiaisenaho. Photon transport physics in Serpent 2 Monte Carlo code. *Comput. Phys. Commun.*, 252:107143, 2020.

[5] Posiva Oy website: https://www.posiva.fi, 2023.

[6] Timothy White, Mikhail Mayorov, Alain Lebrun, Pauli Peura, Tapani Honkamaa, Joakim Dahlberg, Jens Keubler, Victor Ivanov, and Asko Turunen. Application of Passive Gamma Emission Tomography (PGET) for the verification of spent nuclear fuel. In *Proc. 59th Annual Meeting of the Institute of Nuclear Materials Management*, Baltimore, MD, USA, 2018.

[7] Rasmus Backholm, Tatiana A. Bubba, Camille Bélanger-Champagne, Tapio Helin, Peter Dendooven, and Samuli Siltanen. Simultaneous reconstruction of emission and attenuation in passive gamma emission tomography of spent nuclear fuel. *Inverse Problems and Imaging*, 14(2):317–337, 2020.

[8] S. J. Tobin, P. Peura, C. Bélanger-Champagne, M. Moring, P Dendooven, and T Honkamaa. Utility of Including Passive Neutron Albedo Reactivity in an Integrated NDA System for Encapsulation Safeguards. *ESARDA Bulletin*, 56:12–18, 2018.

[9] Topi Tupasela, Peter Dendooven, Stephen J. Tobin, Vladyslav Litichevskyi, Pirkitta Koponen, Asko Turunen, Mikael Moring, and Tapani Honkamaa. Passive neutron albedo reactivity measurements of spent nuclear fuel. *Nucl. Instrum. Meth. Phys. Res. A*, 986:164707, 2021.

[10] Riina Virta, Rasmus Backholm, Tatiana A. Bubba, Tapio Helin, Mikael Moring, Samuli Siltanen, Peter Dendooven, and Tapani Honkamaa. Fuel rod classification from Passive Gamma Emission Tomography (PGET) of spent nuclear fuel assemblies. *ESARDA Bulletin*, 61:10–21, 2020.

[11] Riina Virta, Tatiana A. Bubba, Mikael Moring, Samuli Siltanen, Tapani Honkamaa, and Peter Dendooven. Improved Passive Gamma Emission Tomography image quality in the central region of spent nuclear fuel. *Scientific Reports*, 12(12473), 2022.

[12] John W. Beck, Ronald J. Jaszczak, R. Edward Coleman, C. Frank Starmer, and Loren W. Nolte. Analysis of SPECT including Scatter and Attenuation Using Sophisticated Monte Carlo Modeling Methods. *IEEE Trans. Nucl. Sci.*, 29(1):506–511, 1982.

[13] David R Haynor, Robert L Harrison, and Thomas K Lewellen. The use of importance sampling techniques to improve the efficiency of photon tracking in emission tomography simulations. *Medical Physics*, 18(5):990–1001, 1991.

[14] Jan De Beenhouwer, Steven Staelens, Stefaan Vandenberghe, and Ignace Lemahieu. Acceleration of GATE SPECT simulations. *Medical Physics*, 35(4):1476–1485, 2008.

[15] Freek J Beekman, Hugo WAM de Jong, and Sander van Geloven. Efficient Monte Carlo based reconstruction for general quantitative SPECT. In *2001 IEEE Nuclear Science Symposium Conference Record (Cat. No. 01CH37310)*, volume 4, pages 1864–1868. IEEE, 2001.